Topological Phase Transitions in Multicomponent Superconductors

Topological Phase Transitions in Multicomponent Superconductors

Yuxuan Wang[1] and Liang Fu[2]
[1]Department of Physics and Institute for Condensed Matter Theory, University of Illinois at Urbana-Champaign, 1110 West Green Street, Urbana, Illinois 61801-3080, USA
[2]Department of Physics, Massachusetts Institute of Technology, Cambridge, Massachusetts 02139, USA
(Received 29 June 2017; published 3 November 2017)

We study the phase transition between a trivial and a time-reversal-invariant topological superconductor in a single-band system. By analyzing the interplay of symmetry, topology, and energetics, we show that for a generic normal state band structure, the phase transition occurs via extended intermediate phases in which even- and odd-parity pairing components coexist. For inversion-symmetric systems, the coexistence phase spontaneously breaks time-reversal symmetry. For noncentrosymmetric superconductors, the low-temperature intermediate phase is time-reversal breaking, while the high-temperature phase preserves time-reversal symmetry and has topologically protected line nodes. Furthermore, with approximate rotational invariance, the system has an emergent $U(1) \times U(1)$ symmetry, and novel topological defects, such as half vortex lines binding Majorana fermions, can exist. We analytically solve for the dispersion of the Majorana fermion and show that it exhibits small and large velocities at low and high energies. Relevance of our theory to superconducting pyrochlore oxide $Cd_2Re_2O_7$ and half-Heusler materials is discussed.

DOI: 10.1103/PhysRevLett.119.187003

Introduction.—Topological superconductivity [1–16] offers a unique platform for studying the interplay between topological phases of matter, unconventional superconductivity (SC), and exotic quasiparticle and vortex excitations. In the presence of time-reversal and inversion symmetry, topological superconductors require an odd-parity order parameter (e.g., p wave) [1,17]. Theoretical studies [1,7] proposed that $Cu_xBi_2Se_3$, a doped topological insulator that becomes superconducting below $T_c \sim 3.8$ K, has an odd-parity pairing symmetry favored by the strong spin-orbit coupling in its normal state. Recently, a series of experiments including nuclear magnetic resonance [18], specific heat [19], magnetoresistance [20,21], and torque measurement [22] under a rotating magnetic field have all found that the superconducting state in Cu-, Sr-, and Nb-doped Bi_2Se_3 spontaneously breaks crystal rotational symmetry, only compatible with the time-reversal-invariant p-wave pairing with the E_u symmetry [1,4]. There is currently high interest in searching for the topological excitations in these materials [23–30].

In this Letter, we study topological phase transitions in superconductors resulting from the change of pairing symmetry from even to odd parity. Our study is motivated by a number of experiments showing that pairing interactions in even- and odd-parity channels are of comparable strength in several materials, hereafter referred to as multicomponent superconductors. In the noncentrosymmetric superconductor $Li_2(Pd, Pt)_3B$, the odd-parity spin-triplet, and even-parity spin-singlet pairing components vary continuously as a function of the alloy composition [31–33]. In the pyrochlore oxide $Cd_2Re_2O_7$ [34,35], applying pressure drives phase transitions between different superconducting states, accompanied by an anomalous enhancement of the upper critical field exceeding the Pauli limit [35]. This has been interpreted as a transition from spin-singlet to spin-triplet dominated superconductivity. On the theory side, a pairing mechanism for odd-parity superconductivity in spin-orbit-coupled systems has been recently proposed [36–38], where the pairing interaction arises from the fluctuation of an inversion symmetry breaking order. It was found that this interaction is attractive and nearly degenerate [39–41] in the two fully gapped Cooper channels with s-wave and p-wave symmetry, respectively.

The topology of a superconductor depends crucially on its order parameter, which is in turn determined by energetics. Therefore a change of order parameter as a function of tuning parameters and temperature can result in a topological phase transition in multicomponent superconductors. Furthermore, spontaneous time-reversal-symmetry breaking can be energetically favored in the transition region, thus changing the symmetry that underlies the classification of topological superconductors [42]. Both energetics and spontaneous symmetry breaking need to be taken into account in theory of topological phase transitions in superconductors.

We show that the phase diagram of multicomponent superconductors is largely determined by the fermiology of the normal state, rather than the microscopic pairing mechanism (which is often not exactly known). We find two types of phase diagrams for generic Fermi surfaces with and without inversion symmetry, shown in Figs. 1(b) and 1(d). Remarkably, we find that the transition between the s-wave-dominated trivial phase and the p-wave-dominated topological phase is *generically* interrupted by an extended intermediate phase where s-wave and p-wave pairings

coexist. For superconductors with inversion symmetry, the intermediate phase is a spontaneous time-reversal symmetry breaking (TRSB) and inversion symmetry breaking superconducting state with s-wave and p-wave order parameters differing by a fixed relative phase of $\pm\pi/2$ [43–46]. This $s+ip$ state realizes a superconducting analog of axion insulator [47–50] and exhibits thermal Hall conductance on the surface. For noncentrosymmetric superconductors [51–53], we predict two intermediate phases in the transition region at different temperatures: a time-reversal-invariant phase at temperatures close to T_c and a time-reversal-breaking phase at low temperature. In particular, the time-reversal-invariant phase has topologically protected *line* nodes in the bulk [54,55].

We derive the above results by general considerations of symmetry, topology, and energetics. Important to our analysis is an emergent $U(1)\times U(1)$ symmetry associated with the two phases of $\Delta_\pm \equiv \Delta_s \pm \Delta_p$, where Δ_s and Δ_p are the s-wave and p-wave superconducting order parameters, respectively. In the special case of an isotropic Fermi surface, the $U(1)\times U(1)$ symmetry is exact at the transition between s-wave and p-wave pairing symmetry, and leads to a direct first-order phase transition between trivial and topological superconductors; see Figs. 1(a) and 1(c). In the general case of superconductors with anisotropic Fermi surfaces and gaps, the $U(1)\times U(1)$ symmetry near the topological phase transition is approximate and provides a useful starting point for our theory. Moreover, in this regime, half quantum vortices, which corresponds to the winding of one of the $U(1)$ phases [56], can appear as topological defects, which bind chiral Majorana modes. We solve for the dispersion of the Majorana mode, and show it has a small velocity at zero energy and a large velocity near gap edge.

Our theory is largely independent of specific band structures or pairing mechanisms, and is potentially applicable to a broad range of materials. At the end of this Letter, we discuss the relevance of our general results for the superconducting phases of pyrochlore oxide $Cd_2Re_2O_7$ and half-Heusler compounds, and make testable predictions.

$U(1)\times U(1)$ symmetry.—Throughout this Letter, we assume the system under study has strong spin-orbit coupling. Then single-particle energy eigenstates in the normal state generally do not have well-defined spin. Nonetheless, when both time-reversal and inversion symmetry are present, energy bands remain doubly degenerate at every momentum $\mathbf{k}$, which we label with pseudospin index σ. We choose to work in the manifestly covariant Bloch basis [57], where the state $|\mathbf{k},\sigma=\pm\rangle$ has the same symmetry property as the spin eigenstate $|\mathbf{k},s_z=\uparrow(\downarrow)\rangle$ under the joint rotation of the electron's momentum and spin.

As a convenient starting point, we first consider systems with full rotational invariance. In such systems, all the pairing order parameters can be classified by their total (J) angular momentum. We focus on $J=0$ pairings with a full

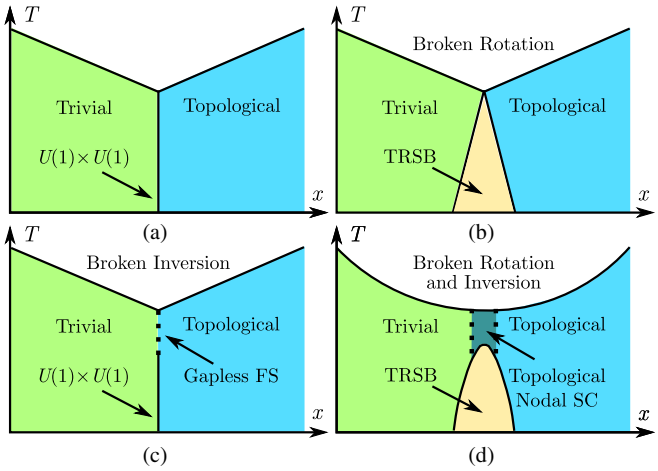

FIG. 1. Schematic phase diagrams near a topological phase transition in multicomponent superconductors with (a),(b) and without (c),(d) inversion symmetry, and with (a),(c) and without (b),(d) rotational symmetry. In (a),(b), the "trivial" phase has an s-wave pairing symmetry and the "topological" phase is p wave. In (c),(d) without inversion symmetry, the topological phase corresponds to the region where the p-wave component is larger. In (c) at the dashed line one of the spin-textured Fermi surfaces is completely gapless, while in (d) in the region between the dashed lines the superconducting states have topologically protected line nodes on the Fermi surface.

gap. If inversion symmetry is present, there are two types of $J=0$ order parameters, with even or odd parity, respectively. The even-parity $J=0$ pairing has s-wave orbital angular momentum given by $\mathcal{H}_s = \Delta_s c^\dagger_{\mathbf{k}} i\sigma^y (c^\dagger_{-\mathbf{k}})^T$, while the odd-parity $J=0$ pairing has p-wave orbital angular momentum given by $\mathcal{H}_p = \Delta_p c^\dagger_{\mathbf{k}} (\hat{\mathbf{k}}\cdot\vec{\sigma}) i\sigma^y (c^\dagger_{-\mathbf{k}})^T$. This p-wave order parameter looks similar to that of the ^{3}He-B phase, but the spin quantization axis is rigidly locked to the momentum by spin-orbit coupling here. In both 2D and 3D, Δ_p realizes time-reversal-invariant topological superconductivity in the DIII class.

We now analyze the interplay between s-wave and p-wave pairings. Generically, the free energy is given by

$$\mathcal{F} = \alpha_1|\Delta_s|^2 + \alpha_2|\Delta_p|^2 + \beta_1|\Delta_s|^4 + \beta_2|\Delta_p|^4 + 4\bar{\beta}|\Delta_s|^2|\Delta_p|^2 + \tilde{\beta}(\Delta_s^2\Delta_p^{*2} + \Delta_p^2\Delta_s^{*2}). \quad (1)$$

The temperature-dependent coefficients α_1, α_2 are determined by the microscopic pairing mechanism. We are interested in the case when s-wave and p-wave instabilities are comparable in strength, i.e., when $\alpha_1 \sim \alpha_2$, so that tuning some parameters such as pressure or chemical composition can drive a phase transition. The interplay between s- and p-wave order parameters is controlled by the β coefficients only. It is important to note that, within weak-coupling theory, β's do not rely on pairing interactions and are completely determined by the normal state electronic

structure, as shown from the Feynman diagram calculation (for details see [58]). Explicitly evaluating these diagrams, we obtain that $\beta_1=\beta_2=\bar{\beta}=\tilde{\beta}\equiv\beta=5\zeta(3)/[8\pi^2T^2N(0)]$, where $N(0)$ is the density of states, and $\zeta(x)$ is the Riemann zeta function.

The last term in (1) is minimized when the phase difference of the two order parameters at $\Delta\phi=\pm\pi/2$. Under this condition, at the phase boundary $\alpha_1=\alpha_2=\alpha$, the free energy (1) becomes

$$\mathcal{F}=\alpha(|\Delta_s|^2+|\Delta_p|^2)+\beta(|\Delta_s|^2+|\Delta_p|^2)^2. \quad (2)$$

This free energy possesses a $U(1)\times U(1)$ symmetry [37] associated with the common phase and relative amplitude of $\Delta_{s,p}$ [62]. When $\alpha_1\neq\alpha_2$, the $U(1)\times U(1)$ symmetry is broken, and the free energy is minimized such that the pairing channel with higher transition temperature (i.e., smaller α) completely suppresses the other, and the phase transition is of first order. Thus we obtain the phase diagram shown in Fig. 1(a). In a previous work [63] it was reported for a rotational invariant system there is a coexistence phase with both s-wave and p-wave orders. Our results differ here, and as we shall see, to obtain the coexistence phase it is necessary to break the rotational invariance, at least within weak-coupling theory.

The emergent $U(1)$ symmetry is a general consequence of the rotational and inversion symmetry of the assumed normal state electronic structure. To see this more explicitly, it is instructive to divide pseoudospin degenerate states on the Fermi surface into two groups, with *helicty* $\chi=\vec{\sigma}\cdot\hat{\mathbf{k}}=\pm1$ separately. Then, the Δ_s and Δ_p order parameters both correspond to pairing within each group of helicity eigenstates (which we denote by $\Delta_\pm$), with constant gap over the Fermi surface as dictated by rotational invariance. The difference of Δ_s and Δ_p is that they are even and odd combinations of $\Delta_\pm$, i.e., $\Delta_{s,p}=(\Delta_+\pm\Delta_-)/\sqrt{2}$ [6,37,64]. In terms of $\Delta_\pm$, the generic free energy (1) can be rewritten as

$$\mathcal{F}=\alpha(|\Delta_+|^2+|\Delta_-|^2)+\delta\alpha(\Delta_+\Delta_-^*+\Delta_+^*\Delta_-)+\beta(|\Delta_+|^4+|\Delta_-|^4), \quad (3)$$

where the coefficients α,β for $\Delta_\pm$ terms are identical due to inversion symmetry which transforms opposite helicity eigenstates into each other, and $\delta\alpha\equiv(\alpha_1-\alpha_2)/2$.

Depending on its sign, $\delta\alpha=\delta\alpha(x)$ controls the relative sign of $\Delta_\pm$ in the ground state, i.e., whether s-wave or p-wave order is favored. In this form the $U(1)\times U(1)$ symmetry is explicit at $\delta\alpha=0$, i.e., the phase boundary of s- and p-wave orders. The "second $U(1)$" can be regarded as a gapless Leggett mode [65] for the relative phase between $\Delta_\pm$.

Time-reversal symmetry breaking phases.—In an actual system without full rotational invariance, the $U(1)\times U(1)$ symmetry is at best approximate. To see this, we still consider s-wave and p-wave pairing orders, $\mathcal{H}_s=\Delta_s f_s(\mathbf{k})c^\dagger_{\mathbf{k}}i\sigma^y(c^\dagger_{-\mathbf{k}})^T$, $\mathcal{H}_p=\Delta_p f_p(\mathbf{k})c^\dagger_{\mathbf{k}}(\hat{\mathbf{k}}\cdot\vec{\sigma})i\sigma^y(c^\dagger_{-\mathbf{k}})^T$, where the form factors $f_{s,p}(\mathbf{k})$ are positive and even functions of $\mathbf{k}$. For weak-coupling superconductivity, $f_{s,p}(\mathbf{k})=f_{s,p}(\hat{\mathbf{k}})$. Since there is no further symmetry requirement restricting them, in general $f_s(\hat{\mathbf{k}})\neq f_p(\hat{\mathbf{k}})$. As a concrete example, we constructed a microscopic model [58] (see also [66]) with instabilities towards both s-wave and p-wave orders.

By computing the β coefficients [58] in Eq. (1) for generic form factors, we find $\bar{\beta}=\tilde{\beta}$ and $\bar{\beta}^2<\beta_1\beta_2$. This indicates a coexistence phase of s-wave and p-wave orders [45]. Thus the first-order transition with $U(1)\times U(1)$ symmetry expands into an intermediate phase. Since Δ_s and Δ_p differs by a phase $\pi/2$, this $s+ip$ state spontaneously breaks time-reversal symmetry [44–46]. Such state in three dimensions has unconventional thermal response described by a axion topological field theory [48,63,67–70]; hence, it can be called an "axion superconductor."

Phase diagram without inversion symmetry.—For spin-orbit-coupled materials without inversion symmetry, the Fermi surface is generally spin split. With rotational symmetry, each spin-split Fermi surface is isotropic and has a definite helicity $\chi=\pm1$. The free energy, written in terms of the order parameters $\Delta_\pm$ on each of the helical Fermi surfaces, takes a general form $\mathcal{F}=\alpha_+|\Delta_+|^2+\alpha_-|\Delta_-|^2+\delta\alpha(\Delta_+\Delta_-^*+\Delta_+^*\Delta_-)+\beta_+|\Delta_+|^4+\beta_-|\Delta_-|^4$. At the phase boundary with $\delta\alpha=0$, the free energy retains an explicit $U(1)\times U(1)$ symmetry. There are two separate transition temperatures, corresponding to the onset of $\Delta_\pm$, respectively. Away from the $\delta\alpha=0$ point, the two order parameters are always mixed down to zero temperature once either one of them becomes nonzero. We thus obtain the phase diagram in Fig. 1(c). For a negative (positive) $\delta\alpha$, Δ_+ and Δ_- take the same (opposite) sign. Switching to $\Delta_{s,p}$ notation, the phase with $\Delta_\pm$ of opposite signs has the p-wave pairing component dominating over the s-wave pairing. This phase is adiabatically connected to the p-wave-only phase in the presence of inversion symmetry, and hence is topological [71].

Finally, with broken rotational symmetry, again the low-temperature first-order transition with $U(1)\times U(1)$ symmetry expands into a time-reversal symmetry breaking phase [58,72], as discussed before. At higher temperatures, $r\equiv\Delta_s/\Delta_p$ is real, and $|r|\gg(\ll)1$ corresponds to a fully gapped trivial (topological) phase. When $r\sim1$, the intermediate phase generally has nodes given by $rf_s(\hat{\mathbf{k}})=\pm f_p(\hat{\mathbf{k}})$, where $\pm$ corresponds to two spin-split Fermi surfaces. It can *only* be satisfied on one of the split Fermi surfaces. The nodes of this intermediate phase have codimension 2 and are isolated points in two dimensions and nodal lines in three dimensions. Time-reversal symmetry further requires that in 3D nodal lines appear in pairs and in

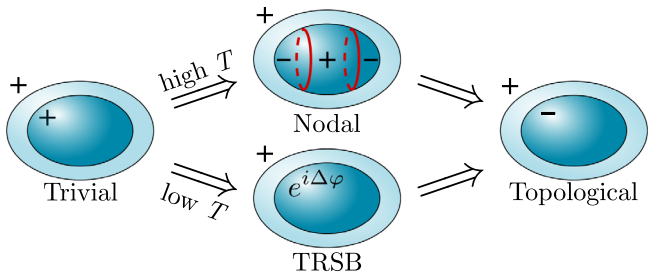

FIG. 2. Transitions between trivial and topological superconductor with only time reversal symmetry [the case of Fig. 1(d)]. In 3D, at high T the transition occurs via intermediate nodal line (nodal points if 2D) superconducting phases, while at low T time-reversal symmetry is spontaneously broken.

2D nodal points in multiples of four (see Fig. 2) [73]. These nodes are topologically protected by a $\mathbb{Z}_2$ invariant [54,55], and lead to flat bands of surface Andreev states [74–76]. The nodal lines are gapped upon entering the time-reversal breaking phase. Time-reversal breaking in nodal line superconductors was obtained in Ref. [77] but only for the surface states; here the time-reversal breaking occurs in the bulk. We summarize the phase diagram in Fig. 1(d).

Experimental consequences.—In the time-reversal-breaking phase, e.g., the $s \pm ip$-SC, the surface state can be thought of as a Majorana cone gapped by the s-wave component [58]. Such a surface state exhibits a thermal Hall effect and polar Kerr effect [68,78].

When rotational symmetry (even when approximate) is present, half quantum vortices, i.e., the phase winding of only one of $\Delta_\pm$ [denoted as $(\pm 1, 0)$ and $(0, \pm 1)$], appear as topological defects because of the $U(1) \times U(1)$ symmetry. The magnetic flux through a half-quantum vortex is given by $hc/(4e)$, i.e., half the flux quantum in a superconductor, hence the name. In 2D, the two helical Fermi surfaces with $\chi = \pm 1$ each enclose a Berry flux of π; hence, their corresponding half-quantum vortex for $\Delta_\pm$ binds a *single* Majorana zero mode with non-Abelian statistics [59,79,80]. This is in contrast with a full vortex in a time-reversal-invariant topological superconductor, which binds two Majorana modes with Abelian statistics.

In 3D, the half quantum vortex line binds a propagating chiral Majorana mode [67,70]. Furthermore, we find that the dispersion $\epsilon = \epsilon(k_z)$ of such a chiral Majorana mode exhibit both slow and fast components. In [58] we perturbatively solve the BdG equation for small $k_z \ll \Delta/v_F$, and show that the dispersion of the chiral Majorana mode is given by $\epsilon(k_z) = v_M k_z$ where

$$v_M(k_z = 0) \approx (\Delta_+/\mu)^2 \log(\mu/\Delta_+) v_F \ll v_F. \quad (4)$$

At larger $k_z \sim k_F$, the 2D Fermi surface slice shrinks and the above perturbative result is no longer valid. The vortex mode becomes higher in energy and merges into the bulk with a much larger velocity $v_M \sim v_F$. Therefore, the

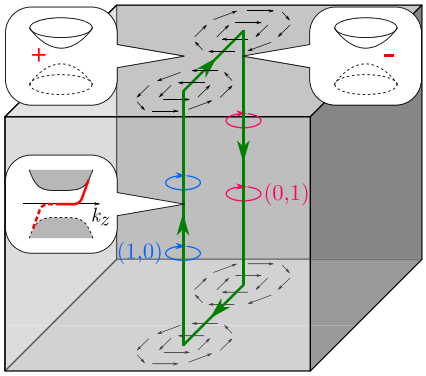

FIG. 3. The chiral Majorana modes (green arrowed lines) bound to and connecting a pair of half vortices (1,0) and (0,1). The surface part of the chiral Majorana mode can be thought of as the chiral edge state at a mass domain wall of the surface Majorana cone. The bulk part of the chiral Majorana mode exhibits a dispersion with both slow and fast modes.

Majorana bound state contains both slow and fast modes, both of which are chiral. We schematically show such a dispersion in the inset of Fig. 3.

Given a pair of opposite half quantum vortices, there exists a pair of chiral Majorana modes on the surface connecting the two vortices. A (0,1) and (1,0) half-quantum vortex pair can be viewed as a vortex-antivortex pair for the relative phase $\Delta\varphi = \varphi_+ - \varphi_-$ between $\Delta_\pm$. Locally, this corresponds to $(1 + e^{i\Delta\varphi})s + (1 - e^{i\Delta\varphi})p$ symmetry. In the slow-varying spatial limit, across the line where $\Delta\varphi = \pi$, locally the surface states are described by two Majorana cones with opposite mass terms [58], shown in Fig. 3. The $\Delta\varphi = \pi$ line acts as a mass domain wall for the Majorana fermions, and thus supports a chiral mode. The chiral Majorana modes bound to the half-quantum vortices and the surfaces form a closed contour, shown in Fig. 3. This chiral Majorana mode is charge neutral and can support thermal transport.

Relation to materials.—Our theory can be applied to systems where even- and odd-parity superconducting order parameters are intertwined, such as $Cd_2Re_2O_7$ and half-Heusler materials. For $Cd_2Re_2O_7$ [34,35], the anomalous enhancement in upper critical field H_{c2} indicates a symmetry change from spin singlet to spin triplet as a function of pressure. Our theory predicts nodal as well as time-reversal-breaking phases near this region in the phase diagram. In half-Heusler superconductors YPtBi [81] and LuPtBi [82], order parameters with mixed even- and odd-parity pairings have been proposed [83,84] to account for penetration depth measurements [81]. This microscopic study finds line nodes in a region of mixed-parity phase, consistent with our general phase diagram for noncentrosymmetric superconductors presented in Fig. 1(d). Our theory further predicts that the superconducting state with line nodes transitions into a new time-reversal breaking phase upon lowering temperatures. It will be interesting

to directly search for this time-reversal symmetry low-temperature phase.

This work was supported by the Gordon and Betty Moore Foundation's EPiQS Initiative through Grant No. GBMF4305 at the University of Illinois (Y. W.) and the DOE Office of Basic Energy Sciences, Division of Materials Sciences and Engineering under Award No. DE-SC0010526 (L. F.). We thank the hospitality of the summer program "Multi-Component and Strongly-Correlated Superconductors" at Nordita, Stockholm, where this work was initiated. Y. W. acknowledges support by the Boulder Summer School for Condensed Matter and Materials Physics through NSF Grant No. DMR-13001648, where part of the work was done.

[1] L. Fu and E. Berg, Phys. Rev. Lett. **105**, 097001 (2010).
[2] M. Kriener, K. Segawa, Z. Ren, S. Sasaki, and Y. Ando, Phys. Rev. Lett. **106**, 127004 (2011).
[3] N. Levy, T. Zhang, J. Ha, F. Sharifi, A. A. Talin, Y. Kuk, and J. A. Stroscio, Phys. Rev. Lett. **110**, 117001 (2013).
[4] L. Fu, Phys. Rev. B **90**, 100509 (2014).
[5] K. Sun, C.-K. Chiu, H.-H. Hung, and J. Wu, Phys. Rev. B **89**, 104519 (2014).
[6] P. M. R. Brydon, S. Das Sarma, H.-Y. Hui, and J. D. Sau, Phys. Rev. B **90**, 184512 (2014).
[7] X. Wan and S. Y. Savrasov, Nat. Commun. **5**, 4144 (2014).
[8] S. Nakosai, Y. Tanaka, and N. Nagaosa, Phys. Rev. Lett. **108**, 147003 (2012).
[9] M. S. Scheurer and J. Schmalian, Nat. Commun. **6**, 6005 (2015).
[10] P. Hosur, X. Dai, Z. Fang, and X.-L. Qi, Phys. Rev. B **90**, 045130 (2014).
[11] N. F. Q. Yuan, K. F. Mak, and K. T. Law, Phys. Rev. Lett. **113**, 097001 (2014).
[12] T. Yoshida, M. Sigrist, and Y. Yanase, Phys. Rev. Lett. **115**, 027001 (2015).
[13] F. Yang, C.-C. Liu, Y.-Z. Zhang, Y. Yao, and D.-H. Lee, Phys. Rev. B **91**, 134514 (2015).
[14] Y. Ando and L. Fu, Annu. Rev. Condens. Matter Phys. **6**, 361 (2015).
[15] M. S. Scheurer, Phys. Rev. B **93**, 174509 (2016).
[16] K. Lee and E.-A. Kim, arXiv:1702.03294.
[17] M. Sato, Phys. Rev. B **81**, 220504 (2010).
[18] K. Matano, M. Kriener, K. Segawa, Y. Ando, and G.-q. Zheng, Nat. Phys. **12**, 852 (2016).
[19] S. Yonezawa, K. Tajiri, S. Nakata, Y. Nagai, Z. Wang, K. Segawa, Y. Ando, and Y. Maeno, Nat. Phys. **13**, 123 (2017).
[20] Y. Pan, A. M. Nikitin, G. K. Araizi, Y. K. Huang, Y. Matsushita, T. Naka, and A. de Visser, Sci. Rep. **6**, 28632 (2016).
[21] G. Du, Y. Li, J. Schneeloch, R. D. Zhong, G. Gu, H. Yang, H. Lin, and H.-H. Wen, Science China Physics, Mechanics & Astronomy **60**, 037411 (2017).
[22] T. Asaba, B. J. Lawson, C. Tinsman, L. Chen, P. Corbae, G. Li, Y. Qiu, Y. S. Hor, L. Fu, and L. Li, Phys. Rev. X **7**, 011009 (2017).
[23] Y. Nagai, H. Nakamura, and M. Machida, Phys. Rev. B **86**, 094507 (2012).
[24] T. Hashimoto, K. Yada, A. Yamakage, M. Sato, and Y. Tanaka, J. Phys. Soc. Jpn. **82**, 044704 (2013).
[25] J. W. F. Venderbos, V. Kozii, and L. Fu, Phys. Rev. B **94**, 180504 (2016).
[26] L. Chirolli, F. de Juan, and F. Guinea, Phys. Rev. B **95**, 201110 (2017).
[27] V. Tien Phong, N. R. Walet, and F. Guinea, Phys. Rev. B **96**, 060505 (2017).
[28] N. F. Q. Yuan, W.-Y. He, and K. T. Law, Phys. Rev. B **95**, 201109 (2017).
[29] F. Wu and I. Martin, Phys. Rev. B **95**, 224503 (2017).
[30] M. P. Smylie, H. Claus, U. Welp, W.-K. Kwok, Y. Qiu, Y. S. Hor, and A. Snezhko, Phys. Rev. B **94**, 180510 (2016).
[31] P. Badica, T. Kondo, and K. Togano, J. Phys. Soc. Jpn. **74**, 1014 (2005).
[32] H. Q. Yuan, D. F. Agterberg, N. Hayashi, P. Badica, D. Vandervelde, K. Togano, M. Sigrist, and M. B. Salamon, Phys. Rev. Lett. **97**, 017006 (2006).
[33] S. Harada, J. J. Zhou, Y. G. Yao, Y. Inada, and G.-q. Zheng, Phys. Rev. B **86**, 220502 (2012).
[34] H. Sakai, K. Yoshimura, H. Ohno, H. Kato, S. Kambe, R. E. Walstedt, T. D. Matsuda, Y. Haga, and Y. Onuki, J. Phys. Condens. Matter **13**, L785 (2001).
[35] T. C. Kobayashi, Y. Irie, J. ichi Yamaura, Z. Hiroi, and K. Murata, J. Phys. Soc. Jpn. **80**, 023715 (2011).
[36] V. Kozii and L. Fu, Phys. Rev. Lett. **115**, 207002 (2015).
[37] Y. Wang, G. Y. Cho, T. L. Hughes, and E. Fradkin, Phys. Rev. B **93**, 134512 (2016).
[38] J. Ruhman, V. Kozii, and L. Fu, Phys. Rev. Lett. **118**, 227001 (2017).
[39] S. Lederer, Y. Schattner, E. Berg, and S. A. Kivelson, Phys. Rev. Lett. **114**, 097001 (2015).
[40] J. Kang and R. M. Fernandes, Phys. Rev. Lett. **117**, 217003 (2016).
[41] Y. Wang and A. V. Chubukov, Phys. Rev. B **92**, 125108 (2015).
[42] S. Ryu, A. P. Schnyder, A. Furusaki, and A. W. W. Ludwig, New J. Phys. **12**, 065010 (2010).
[43] W.-C. Lee, S.-C. Zhang, and C. Wu, Phys. Rev. Lett. **102**, 217002 (2009).
[44] S. Maiti and A. V. Chubukov, Phys. Rev. B **87**, 144511 (2013).
[45] Y. Wang and A. Chubukov, Phys. Rev. B **90**, 035149 (2014).
[46] A. Hinojosa, R. M. Fernandes, and A. V. Chubukov, Phys. Rev. Lett. **113**, 167001 (2014).
[47] X.-L. Qi, T. L. Hughes, and S.-C. Zhang, Phys. Rev. B **78**, 195424 (2008).
[48] A. M. Essin, J. E. Moore, and D. Vanderbilt, Phys. Rev. Lett. **102**, 146805 (2009).
[49] X. Wan, A. Vishwanath, and S. Y. Savrasov, Phys. Rev. Lett. **108**, 146601 (2012).
[50] Z. Wang and S.-C. Zhang, Phys. Rev. B **87**, 161107 (2013).
[51] K. V. Samokhin and V. P. Mineev, Phys. Rev. B **77**, 104520 (2008).
[52] K. Samokhin, Ann. Phys. (Amsterdam) **359**, 385 (2015).
[53] M. Smidman, M. B. Salamon, H. Q. Yuan, and D. F. Agterberg, Rep. Prog. Phys. **80**, 036501 (2017).
[54] K. Shiozaki and M. Sato, Phys. Rev. B **90**, 165114 (2014).

[55] C.-K. Chiu and A. P. Schnyder, Phys. Rev. B **90**, 205136 (2014).
[56] E. Babaev, Nucl. Phys. **B686**, 397 (2004).
[57] L. Fu, Phys. Rev. Lett. **115**, 026401 (2015).
[58] See online Supplemental Material at http://link.aps.org/supplemental/10.1103/PhysRevLett.119.187003, which include Refs. [36,37,44,59–61], for details.
[59] L. Fu and C. L. Kane, Phys. Rev. Lett. **100**, 096407 (2008).
[60] A. J. Leggett, Rev. Mod. Phys. **47**, 331 (1975).
[61] D. Vollhardt and P. Wölfle, *The Superfluid Phases of Helium 3* (Taylor & Francis, London, England, 1990).
[62] Note that he additional $U(1)$ is *not* the rotational symmetry we impose, but rather is emergent.
[63] P. Goswami and B. Roy, Phys. Rev. B **90**, 041301 (2014).
[64] K. Michaeli and L. Fu, Phys. Rev. Lett. **109**, 187003 (2012).
[65] A. J. Leggett, Prog. Theor. Phys. **36**, 901 (1966).
[66] C. Wu and J. E. Hirsch, Phys. Rev. B **81**, 020508 (2010).
[67] X.-L. Qi, E. Witten, and S.-C. Zhang, Phys. Rev. B **87**, 134519 (2013).
[68] S. Ryu, J. E. Moore, and A. W. W. Ludwig, Phys. Rev. B **85**, 045104 (2012).
[69] K. Shiozaki and S. Fujimoto, Phys. Rev. B **89**, 054506 (2014).
[70] M. Stone and P. L. e S. Lopes, Phys. Rev. B **93**, 174501 (2016).
[71] X.-L. Qi, T. L. Hughes, and S.-C. Zhang, Phys. Rev. B **81**, 134508 (2010).
[72] C. Setty, Y. Wang, and P. W. Phillips, Phys. Rev. B **96**, 054508 (2017).
[73] B. Béri, Phys. Rev. B **81**, 134515 (2010).
[74] A. P. Schnyder and P. M. R. Brydon, J. Phys. Condens. Matter **27**, 243201 (2015).
[75] P. M. R. Brydon, A. P. Schnyder, and C. Timm, Phys. Rev. B **84**, 020501 (2011).
[76] A. P. Schnyder and S. Ryu, Phys. Rev. B **84**, 060504 (2011).
[77] C. Timm, S. Rex, and P. M. R. Brydon, Phys. Rev. B **91**, 180503 (2015).
[78] R. Nakai, S. Ryu, and K. Nomura, Phys. Rev. B **95**, 165405 (2017).
[79] G. Moore and N. Read, Nucl. Phys. **B360**, 362 (1991).
[80] D. A. Ivanov, Phys. Rev. Lett. **86**, 268 (2001).
[81] H. Kim, K. Wang, Y. Nakajima, R. Hu, S. Ziemak, P. Syers, L. Wang, H. Hodovanets, J. D. Denlinger, P. M. R. Brydon, D. F. Agterberg, M. A. Tanatar, R. Prozorov, and J. Paglione, arXiv:1603.03375.
[82] Z. K. Liu, L. X. Yang, S. C. Wu, C. Shekhar, J. Jiang, H. F. Yang, Y. Zhang, S. K. Mo, Z. Hussain, B. Yan, C. Felser, and Y. L. Chen, Nat. Commun. **7**, 12924 EP (2016).
[83] P. M. R. Brydon, L. Wang, M. Weinert, and D. F. Agterberg, Phys. Rev. Lett. **116**, 177001 (2016).
[84] W. Yang, Y. Li, and C. Wu, Phys. Rev. Lett. **117**, 075301 (2016).